REVIEW ARTICLE | APRIL 29 2026

From growth to integration: Quantum dot devices for quantum photonics

Special Collection: Quantum Light

Tobias Huber-Loyola ; Andreas Theo Pfenning ; Johannes Michl ; Sven Höfling

Appl. Phys. Rev. 13, 021318 (2026)
https://doi.org/10.1063/5.0287406

Applied Physics Reviews REVIEW pubs.aip.org/aip/are

From growth to integration: Quantum dot devices for quantum photonics

Cite as: Appl. Phys. Rev. **13**, 021318 (2026); doi: 10.1063/5.0287406
Submitted: 24 June 2025 · Accepted: 3 April 2026 ·
Published Online: 29 April 2026

Tobias Huber-Loyola,[1,a)] Andreas Theo Pfenning,[2] Johannes Michl,[2] and Sven Höfling[2]

AFFILIATIONS

[1]Karlsruhe Institute of Technology, Institute of Photonics and Quantum Electronics & Center for Integrated Quantum Science and Technology, Karlsruhe, Germany
[2]Julius-Maximilians-Universität Würzburg, Lehrstuhl für Technische Physik, Würzburg, Germany

Note: This paper is part of the Special Topic, Quantum Light.
[a)]**Author to whom correspondence should be addressed:** tobias.huber-loyola@kit.edu

ABSTRACT

Semiconductor quantum dots represent one of the most promising classes of deterministic single-photon sources for emerging quantum technologies. These nanostructures offer several key advantages, including extremely low multi-photon emission probabilities, high photon fluxes, and the potential for large-scale production using well-established semiconductor fabrication techniques. Their operation has been thoroughly demonstrated in the visible and near-infrared spectral regions, and considerable effort is now focused on adapting these devices to emit within the telecommunication wavelength bands. Achieving this compatibility is an essential milestone toward realizing fiber-integrated quantum communication networks. This review provides an overview of various methods for the growth of quantum dots, alongside strategies implemented at the device level to improve their optical performance across a range of emission wavelengths. A particular emphasis is placed on work conducted by the Chair of Technische Physik at the University of Würzburg, but we do present our work in the broader context of other approaches. We examine major advancements in epitaxial growth techniques on indium phosphide (InP) substrates, as well as innovations in mechanical strain tuning using piezoelectric elements, and photonic integration via micropillar cavities and circular Bragg grating structures. Furthermore, we discuss recent progress in enhancing photon indistinguishability within the telecom C-band using advanced excitation schemes and cavity quantum electrodynamics, including efforts in deterministic cavity positioning. Collectively, these developments underscore the strong potential of quantum dot-based devices as foundational components for scalable, high-performance quantum photonic systems.

TABLE OF CONTENTS

INTRODUCTION 1
Historical overview of quantum dots 2
Growth of quantum dots: Stranski–Krastanov (SK), droplet epitaxy (DE), local droplet etching (LDE) . . . 3
Nanophotonic structures. 5
Outlook: Co-design, integration, and scaling of telecom-band quantum dot photonics. 7
CONCLUSION. 10

INTRODUCTION

Quantum light sources are a central building block of photonic quantum technologies that enable secure communication, quantum networks, quantum-enhanced sensing, networked quantum computing, and quantum metrology.[1–3] An ideal source should emit single photons on demand with high efficiency, high indistinguishability, and minimal multiphoton contributions. Among various platforms, semiconductor quantum dots (QDs) stand out by combining atom-like optical properties with scalable fabrication and integration.[4] They can emit single[5,6] or entangled photons[7,8] and can be engineered to emit across a broad spectral range, from the visible[4,9] to the telecom bands.[10,11] This can be achieved by changing material composition or by employing strain compensation during crystal growth. Over the past decade, advances in growth techniques, charge control, and photonic design have transformed quantum dots into highly optimized single-photon sources. Developments like cavity-enhanced emission and resonant excitation have pushed performance toward the ideal

photon emission. Furthermore, site-controlled growth[12–15] combined with spectral tuning techniques for quantum dots[16–19] promises future spatially and spectrally scalable fabrication. There is a wide range of recent review and perspective papers on semiconductor quantum dots and their role in quantum photonic applications. We refer the interested reader to Refs. 1–3 and 20–23 for comprehensive reviews on this topic.

One aspect of quantum dots for applications that has not been extensively covered is that by using precisely timed optical excitation of spins in semiconductor quantum dots, linear photonic cluster states can be generated,[24–27] reducing the resource overhead for fault-tolerant optical quantum computing.[28] For fault tolerant quantum computing, the 6-ring graph state, see Fig. 1, can be a resource state. Indeed, a combinatorial resource estimate shows that multiplexing fewer than 100 quantum dot single-photon sources can achieve fault-tolerant computing, considering current system efficiencies.[29] Prasad *et al.* developed an algorithm[30] that calculates linear cluster state fidelities, considering errors such as spin decoherence and finite excited state lifetime. They find that partial reinitialization with each photon emission mitigates the coherence time limitation, whereas the error introduced by the excited state lifetime can be mitigated by Purcell enhancement. Near-unity fidelities for 3- and 7-photon linear cluster states are achievable with state-of-the-art quantum dots.[30] In general, graph states with a specific topology, like 6-ring graph states or quantum repeater graph states,[31] see Fig. 1, are of great interest for quantum computing[32] and memory-free quantum repeaters.[33] Depending on the chosen encoding, certain devices are more or less suitable for generating such states. The original proposal by Lindner and Rudolf[25] and all demonstrated experimental implementations[24,26,27,34] choose polarization encoding for the creation of linear cluster states, which can later be fused to the states of interest,[35] however, proposals for cluster-states using time-bin encoding exist.[36,37] For polarization encoding, nanophotonic devices that do not introduce polarization bias are needed. The circular Bragg grating (CBG), or bullseye, resonator is a good choice to fulfill this requirement, see Fig. 1, and more details in the section nanophotonic devices. In this review, we discuss growth and tuning strategies, and then examine nanophotonic structures for improved light extraction and photon coherence. We discuss electrical control and deterministic device fabrication, and we will conclude with an outlook on future developments.

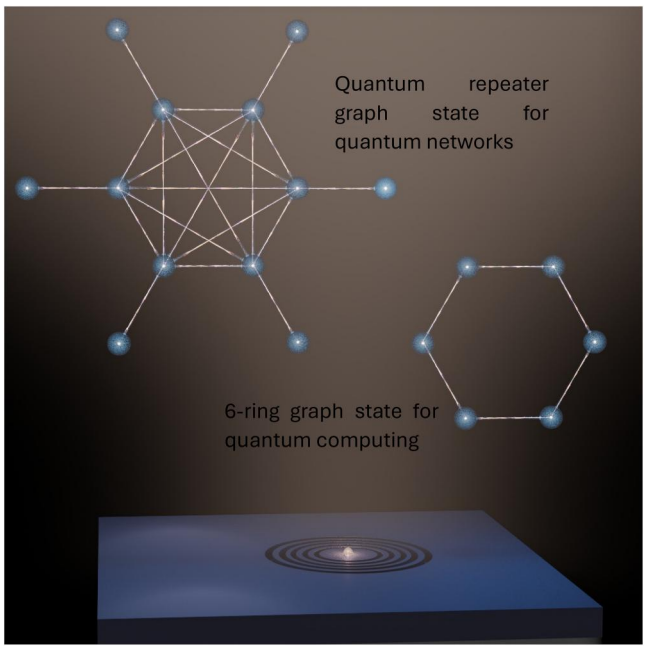

FIG. 1. Quantum dots embedded in a circular Bragg grating resonator (CBG) can produce polarization encoded graph states that can be fused to states that are useful for quantum computing and quantum repeaters.

Before diving into the review, we would like to define some of the above-mentioned metrics in Table I, so that all readers are on the same page.

Historical overview of quantum dots

The past 50 years have shown an astonishing progress from the first experimental demonstration of quantum dots to their integration into complex nanophotonic structures, utilizing these "artificial atoms" as on demand sources for quantum light. This section aims to provide a short timeline of the milestones in quantum dot growth and processing as an overview, placing them in the relevant decades, without the claim to be a complete historic review. In Fig. 2, we give a graphical overview over these events.

With the invention of molecular-beam-epitaxy (MBE) in the late 1960s, the door was opened to fabricating heterostructures with monolayer precision. This precise control over the confinement in one direction (along the growth axis) produced novel optoelectronic devices like lasers.[41] With their work in the early 1980s, Ekimov and Onushchenko were the first to demonstrate confinement in all three spatial dimensions, although not with epitaxially grown material but for nanocrystals in a transparent dielectric matrix.[42] For the first demonstration of "quantum dots," Ekimov was awarded the Noble Price for Chemistry in 2023. Advantages of quantum dots for semiconductor lasers have already been proposed by Arakawa and Sakaki in 1982.[43] High crystalline quality of 3D islands in InAs/GaAs superlattices has already been shown in 1985.[44] The first self-assembled quantum dots grown by MBE have been reported in the 1990s for highly strained InGaAs on GaAs,[45] with a dot density that reached values as high as $10^{11}\,\mathrm{cm}^{-1}$. A TEM image from the referenced study by Leonard *et al.*, shown in Fig. 2, illustrates this high density. As a consequence, the optical characterization was performed primarily through ensemble emission measurements rather than single-dot analysis. The switch to collecting photoluminescence from single dots can be placed around the turn of the millennium, when e.g., Becher *et al.*[46–48] performed second-order autocorrelation measurements in a Hanbury Brown—Twiss configuration and could show a $g^{(2)}(0) < 0.5$, which was soon adapted as a benchmark for single quantum dots.

Since then, research has focused to a large part on fabricating nanophotonic resonators around single quantum dots to boost extraction efficiency and harness the reduced radiative lifetime, a direct consequence of the Purcell effect. Since different resonator designs are discussed in this review in detail at a later point, Fig. 2 only roughly maps three cavity platforms that have gained much interest in the past 25 years and have been chosen depending on the primary objective. Photonic crystal cavities were central in the early 2000s for exploring strong light–matter coupling[49,50] and solid-state cavity

TABLE I. Definition of metrics, how they are used by the community and by us in this review.

Metric	Definition	Typical measurement
On demand	Pulsed excitation of a quantum dot prepared in a controlled charge state, so a photon is emitted in a predefined time window	System efficiency: measured using calibrated detectors Sometimes, only on-demand preparation: measured through Rabi oscillations
Extraction efficiency	Probability that an emitted photon exits the device into the target optical mode; independent of detection losses	Calculated from power radiated into the mode or inferred from corrected count rates
System efficiency	Product of excitation probability, extraction efficiency, and optical/detector transmission	Total counts at the output fiber divided by the excitation repetition rate Mostly not reported, unless very high, c.f. Refs. 38 and 39
Indistinguishability	Degree to which two photons are identical in energy, temporal envelope, and polarization; measured via HOM visibility	HOM visibility V, comparing integrated (sometimes post selected) center peak to orthogonal control measurement
Multi-photon contribution	Probability of emitting more than one photon per pulse, assessed via the second-order autocorrelation $g^{(2)}(0)$	$g^{(2)}(0)$ measurement with Hanbury Brown–Twiss measurement Expected to be close to zero in a two-level system, depends on excitation scheme, but can be spoiled by leakage of excitation laser or other emitters nearby. The best values are achieved in two-photon excitation schemes[40]

quantum electrodynamics (QED),[51] while micropillar resonators became the workhorse for generating bright, highly indistinguishable single photons, with reported extraction efficiencies around 70%.[5,52,53] On the latter, piezo tuning[17] and electrical contacting[54] have also been implemented.

More recently, circular Bragg grating (bullseye) cavities and related designs have gained much attention for their high Purcell factors, broadband extraction efficiency and suitability for scalable, fiber-coupled quantum photonic devices. Their numerically predicted extraction efficiency is above 90% into a high numerical aperture.[6] Here, too, concepts for electrical contacting have been explored and implemented, and the important shift to the telecommunication C-band wavelength window has been successfully conducted.[55–58]

Growth of quantum dots: Stranski–Krastanov (SK), droplet epitaxy (DE), local droplet etching (LDE)

An optically active semiconductor quantum dot is formed when a low bandgap semiconductor is encapsulated in all three spatial dimensions by a higher bandgap semiconductor and when the two semiconductors have a type-I band alignment. Type-I band alignment means that both, the conduction band and the valence band form an attractive potential in the QD region. This can be achieved by chemical synthesis of core–shell quantum dots[59] or through epitaxial crystal growth in either molecular beam epitaxy or metal-organic vapor-phase epitaxy. We will focus only on epitaxially grown quantum dots and want to distinguish two major types of growth mechanisms: strain driven quantum dot formation and quantum dot growth in lattice matched systems, see Fig. 3. Strain-driven quantum dot formation, the so-called Stranski–Krastanov (SK) growth, is governed by a lattice constant mismatch of the quantum dot material (the low-bandgap semiconductor) and the surface it is grown on (the high-bandgap semiconductor). After a critical thickness, which depends on the strain, but is in general, on the order of a few monolayers, the strain that is built up in the layer is released through the formation of small islands, i.e., the quantum dots. To form a quantum dot, these little islands need to be overgrown with the high-bandgap semiconductor material, after which a three-dimensional confinement is established. Indium arsenide (InAs) has about 7% lattice mismatch with gallium arsenide (GaAs), which forms SK quantum dots that emit between 880 and 1100 nm.[60] To narrow the distribution of quantum dot sizes, a commonly used technique called partial capping and annealing is employed, where the quantum dot is overgrown with GaAs up to a certain thickness, and then the tip of the quantum dot is removed by flushing the growth chamber with arsenic. This creates a quantum dot with a well-defined height to emit light in the 880–970 nm wavelength range.[61]

If one wants to shift the quantum dot formation to longer wavelengths, i.e., the telecom O-band (1260–1360 nm) or the telecom C-band (1530–1565 nm), which are wavelengths that are relevant for telecommunication purpose using fibers, the strain during growth has to be engineered. For O-band quantum dots, a strain relieving layer above the quantum dots can be utilized. For the telecom C-band, the strain has to be engineered before the quantum dot formation, such that larger quantum dots form. This can be achieved by growing lattice matched to indium phosphide (InP), either directly by embedding the (InAs) quantum dots into InP,[62–65] growth on miscut InP substrates,[66–68] although these studies were mostly investigating high density quantum dots for laser applications, by lattice matching InGaAlAs to InP[57] or by growing a InGaAs metamorphic buffer on GaAs.[69,70]

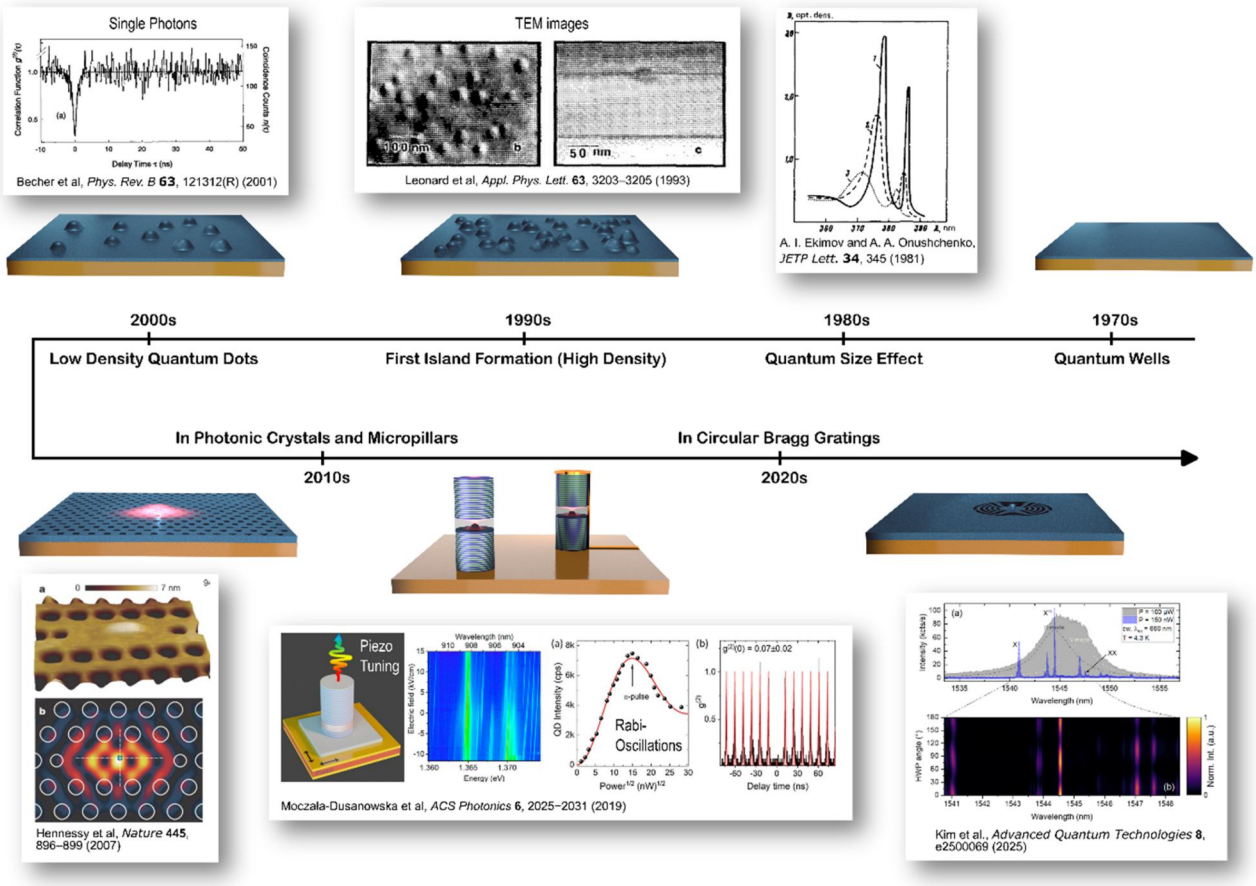

FIG. 2. Short overview of some milestones in the development of quantum dots integrated into nanophotonic resonators, with snapshots from seminal publications. 1970s: Pioneering works in semiconductor superlattices and quantum well physics, facilitated by monolayer growth-control through MBE. 1980s: Discovery of the quantum size effect of nanocrystals in glass, birth of quantum dots. 1990s: First self-assembled quantum dots grown by MBE, measurements of ensemble emission. 2000s: First works on nonclassical light from single quantum dots, low multi-photon contributions shown by $g^{(2)}(0)$ measurements. 2010s: Embedding single quantum dots in photonic resonators. Exploration of different concepts like photonic crystals and micropillars. Piezoelectric tuning and resonant, coherent excitation were shown using micropillars, together with very low multi-photon contributions. 2020s: Novel resonator designs focused on CBGs. The broadband Purcell-enhancement facilitates boosting the emission of more than one radiatively recombining charge carrier. First concepts of electrical contacting have been shown using bridged gaps. (a) Reproduced with permission from A. I. Ekimov and A. A. Onushchenko, JETP **34**, 363 (1981). Copyright 1981 Russian Academy of Science.[42] (b) Reproduced from Leonard *et al.*, Appl. Phys. Lett. **63**, 3203–3205 (1993) with the permission of AIP publishing.[45] (c) Reproduced with permission from Becher *et al.*, Phys. Rev. B **63**, 121312 (2001). Copyright 2001 American Physical Society.[46] (d) Reproduced with permission from Hennessy *et al.*, Nature **445**, 896–899 (2007). Copyright 2007 Springer Nature Publishing.[50] (e) Reproduced with permission from Moczała-Dusanowska *et al.*, ACS Photonics **6**, 2025–2031 (2019). Copyright 2019 American Chemical Society.[17] (f) Reproduced with permission from Kim *et al.*, Adv. Quantum Technol. **8**, e2500069 (2025). Copyright 2025 Authors licensed under a Creative Commons Attribution (CC BY) License.

When growing quaternary alloys, it can happen that indium forms nano-scale clusters, which can be avoided by digital alloying.[71–73] In digital alloying, single layers of ternary InGaAs and InAlAs are stacked on each other, such that the overall material composition is InGaAlAs.

An alternative approach is to grow on lattice matched systems. Since here the quantum dot formation is clearly not strain driven, SK growth cannot be considered. To form quantum dots in such a scenario, different growth techniques, such as droplet epitaxy and local droplet etching (LDE) have been developed.[9] In both cases, a metallic droplet is deposited on the surface of the substrate by removing the flux of the group V element. In droplet epitaxy, this droplet is converted to a III/V semiconductor by offering the group V element in the correct temperature and pressure range, such that the metallic droplet absorbs the group V element and freezes into a quantum dot. In LDE, the group V element is offered in a different temperature and pressure window, such that the metal starts consuming the material under it, leaving a hole behind. This hole can then be filled with a material of choice, forming the quantum dot. In both scenarios, the quantum dot has to be overgrown with the substrate material to achieve three-dimensional confinement.

InAs quantum dots grown on GaAs substrates represent a well-established material platform for emission in the near-infrared (NIR) spectral range, typically between 900 and 960 nm. Over the past years,

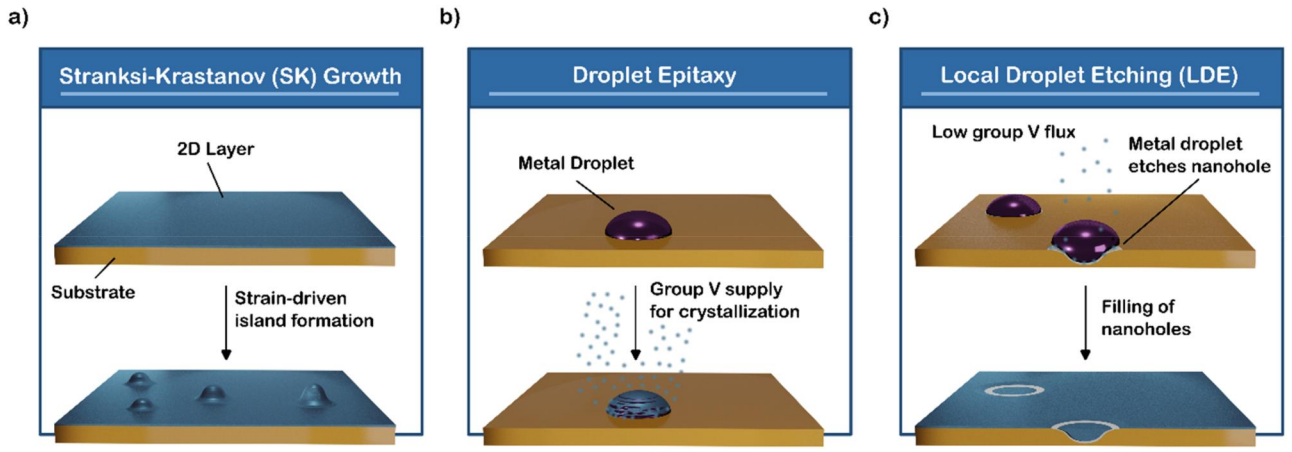

FIG. 3. Various growth modes for quantum dot formation. (a) In Stranski–Krastanov growth, the strain in the grown 2D layer, which comes from lattice mismatch, relaxes after a critical thickness to form quantum dots. (b) In droplet epitaxy, group III metal droplets are forming on the surface and are crystallized in a second step by supplying group V elements. (c) In local droplet etching, a low background pressure destabilizes the interface under the deposited group III metal droplet and leads to etching of holes into the substrate. Quantum dots are formed by filling the nanoholes with III/V semiconductors.

only very few advances in the underlying growth physics have been reported,[74] and the relevant mechanisms have been extensively reviewed elsewhere.[1,4,75,76] Consequently, a detailed discussion of the basic growth processes is omitted here. Nevertheless, this material system remains highly relevant for device development due to its maturity, reproducibility, and well-characterized optical and electronic properties, which provide a robust foundation for nanophotonic integration.

For operation in telecommunication wavelength bands, InAs quantum dots can be realized on InP substrates using quaternary barrier materials such as $In_{0.53}Ga_{0.23}Al_{0.24}As$. In this context, digital alloying of the ternary compounds $In_{0.52}Al_{0.48}As$ and $In_{0.53}Ga_{0.47}As$ has proven advantageous.[57] In digital alloying, individual monolayers of the ternary materials are alternated during growth to approximate the desired quaternary composition.[72] Although the resulting crystal is not electronically identical to a stochastic alloy, photoluminescence measurements indicate that its properties closely match calculations based on the averaged quaternary material parameters. The primary requirement is the formation of a sufficiently large bandgap barrier to ensure strong carrier confinement in the InAs quantum dots; small deviations in the electronic structure are generally not critical for quantum dot formation. More decisive is the surface composition on which the quantum dots nucleate, since indium adatom migration depends sensitively on the local chemical environment. Digital alloying allows controlled selection of the topmost surface layer ($In_{0.52}Al_{0.48}As$ or $In_{0.53}Ga_{0.47}As$), thereby improving reproducibility of growth conditions.[57]

Optimization of the quantum dot emission wavelength can be achieved by systematically varying the deposited material thickness. One approach involves interrupting substrate rotation during quantum dot growth, thereby creating a thickness gradient across the wafer. By correlating local material thickness with emission wavelength, the optimal deposition parameters for a target wavelength—such as the telecom C-band—can be identified and transferred to subsequent growth runs. The optical quality of such telecom quantum dots, quantified by the emission linewidth, is not yet Fourier-limited (i.e., not solely determined by the spontaneous decay rate). However, reported linewidths of $\Delta E_{FWHM} = (28.9 \pm 0.7)\ \mu eV$ are among the best values achieved for Stranski–Krastanov quantum dots in this wavelength regime.[57]

Beyond planar Stranski–Krastanov growth, alternative approaches include bottom-up nanowire growth with embedded quantum dot segments[77–79] and various implementations of site-controlled quantum dot growth,[15] which enable deterministic positioning and integration into photonic architectures. Droplet epitaxy (DE) and local droplet etching (LDE) provide additional strain-independent routes to quantum dot formation. DE typically operates at comparatively low growth temperatures, which can limit material quality,[9] although excellent optical properties have nonetheless been demonstrated.[80] LDE evolved as an extension of DE: a metallic droplet locally etches a nanohole into the substrate, which is subsequently filled with quantum dot material. This method enables the growth of GaAs quantum dots on AlGaAs[81] and GaSb quantum dots on AlGaSb.[82] In particular, GaAs quantum dots fabricated by LDE have shown highly promising results for spin-based quantum applications,[83–86] whereas GaSb-based systems remain comparatively less explored.[82,87,88]

Nanophotonic structures

Although III/V epitaxial quantum dots have many benefits as photon sources, such as a large dipole moment, addressable spin states through optical selection rules, wavelength tunability in growth through material composition and size, compatibility with industrial semiconductor processing, and so forth, they still present two major drawbacks. The first is that their binding energy is small, such that their properties cannot be fully used at room temperature, forcing experiments to be performed at liquid helium temperature. The second drawback is that III/V semiconductors have high optical refractive indices. While this is also a feature when integrating devices that allow for small on-chip bend radii, when collecting light into free space, it is a major challenge. Most of the light remains confined

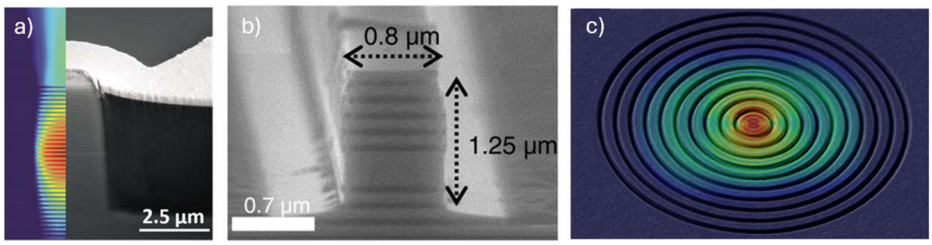

FIG. 4. Nanophotonic structures: (a) scanning electron microscope (SEM) image of an electrically contacted micropillar with electric field simulation overlay. The left side of the image is an electric field simulation that shows the standing wave in the resonator with a high electric field in the center (red) and emission to the top, which is not a standing wave (smooth electric field vs ripples (standing wave) inside the resonator. The right side shows top and bottom DBR out of AlAs and GaAs in the dark and light gray, respectively. The almost white region is a gold ring contact used to electrically contact the device. (b) SEM image of single mode DBR ridge waveguide for integrated photonics. The light is confined in the waveguide to the top and bottom through DBR mirrors, as in (a), and in-plane through the high refractive index contrast between the semiconductor and air. In such a structure, the light emitted from the quantum dot is used in-plane, i.e., in the waveguide instead of coupling it out to the top. (c) SEM image of circular Bragg grating resonator (CBG) with simulated electric field distribution overlay. The CBG consists of etched trenches (dark) and leftover material (brighter). Here, the shown electric field is calculated in the plane of the resonator, which is the main direction responsible for the confinement of the light. In the in-plane electric field component, the outcoupling to the top is not directly visible. (a) Reproduced from Heindel *et al.*, Appl. Phys. Lett. **96**, 011107 (2010) with the permission of AIP Publishing.[89]

within the substrate by total internal reflection, which necessitates the use of nanophotonic structures.

A nanophotonic structure, in general, modifies the electromagnetic environment around the quantum dot, aiming at light collection into a defined mode and eventually changing their decay properties. For some examples of fabricated nanophotonic structures and their simulated field distributions, see Fig. 4. Nanophotonic structures can either be waveguiding structures that reduce the number of modes that are available to couple to, which usually do not alter the decay dynamics, but can lead to high collection efficiency.[90,91] On the other hand, a nanophotonic structure could be a cavity. When coupling emitters to cavities, there are two main regimes, the weak[92] and the strong coupling[49,93] regime. In the weak coupling regime, the decay rate of the quantum dot is modified through the Purcell effect[94] and the emission is funneled into the cavity mode. In the strong coupling regime, the emitted photon does not leave the cavity right away but is likely to be reabsorbed by the emitter. This leads to new eigenmodes, the so-called polaritons.[95]

For controlling the light–matter coupling, mostly three different approaches are used to define nanophotonic cavities. The first, more established approach uses a cavity layer in between two highly reflective distributed Bragg reflectors (DBR), the second approach is the CBG, and the third approach is based on photonic crystals.[96,97] They are an alternative way to confine and direct the propagation of light. They combine low mode volumes with high quality factors[98] in defect-mode cavities showing strong[49,99,100] and weak[51,101] light–matter coupling regime. In addition to cavities, photonic crystals arrangements can be utilized to define waveguides[102,103] and therewith provide a wide toolbox for quantum integrated photonic circuitry and functionality on-chip,[4,100,104,105] including operation wavelengths in the telecommunication regime.[22,103,106]

Micropillars consist of etched DBRs that are composed of layers that are a quarter of a wavelength thick, and one typically uses two different materials with a refractive index difference that is high. The higher the refractive index difference, the wider the reflective bandwidth of the mirror, and the fewer layer pairs one needs for achieving the same reflectivity. In III/V semiconductor, the DBR pairs can be epitaxially grown and often consist of AlAs and GaAs pairs. Often the AlAs layer has a small percentage of Ga intermixed, which makes the refractive index difference a bit worse, but it prevents oxidation of the layer. By changing the amount of DBR pairs, the reflectivity of the mirror can be modified and thus either symmetrical or highly directive cavities can be produced. To make the mode volume better defined and smaller, which helps with the Purcell effect, micropillars are defined through dry-chemical etching.[107] The micropillars interface between the semiconductor and air adds lateral confinement to the structure. It was believed that one needs rather high cavity quality factors (Q) to achieve any reasonable cavity performance, but if outcoupling efficiency is the only metric of interest, i.e., no or very weak Purcell enhancement is acceptable, low-Q micropillars can perform surprisingly well.[108] Here, the lateral confinement forms a very weak Fabry–Pérot resonator, which, if tuned out of resonance, suppresses the quantum dots' coupling to lateral modes, effectively boosting its efficiency into the wanted out-of-plane cavity mode from the low-Q micropillar. Other modifications for low-Q modified micropillar structures with even higher outcoupling efficiency[109] turned out to be rather challenging.[110] Such low-Q micropillars are broadband enough to enhance the efficiency of the biexciton and exciton line simultaneously, which allows for the efficient collection of entangled photon pairs.[111]

In addition to growing the DBR epitaxially out of III/V semiconductor, one could also think about depositing dielectric DBR mirrors on top of an epitaxial structure, which has a bottom III/V DBR, or even dielectric DBRs on both sides. While such dielectric structures make post-processing harder, due to the needed change in chemistry, cavities can be defined before the top mirror deposition.[112] Especially in strained systems, such as after growing metamorphic buffers to shift the quantum dot energy into the telecom C-band,[70] the growth of III/V DBRs becomes very challenging, and the use of dielectric DBRs offers a solution to still define nice cavity modes. Even without nano-structuring, a planar DBR cavity can boost the extraction efficiency of the photons, enabling enough photon flux for challenging quantum storage[113] or spin-control experiments.[114,115]

One design of resonator structure that gained a great deal of attention in the community is the CBG.[118,119] This resonator has a rather easy design in growth and offers high Purcell factors and high outcoupling efficiency over a broad wavelength range, making it very attractive for embedding solid state emitters. The broad wavelength

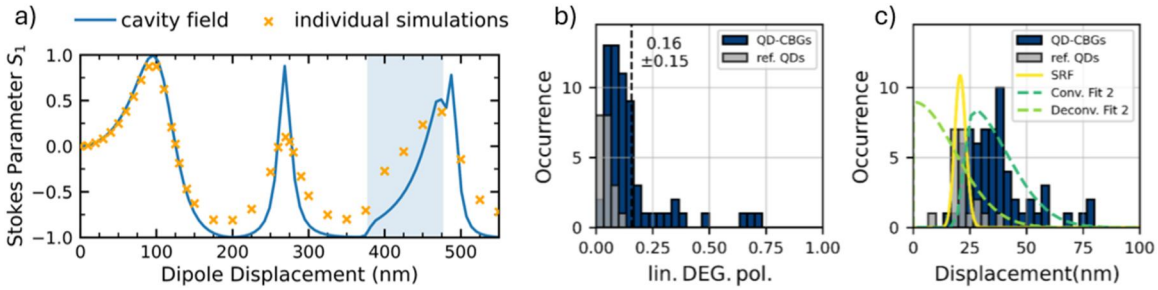

FIG. 5. (a) Polarization dependence on displacement; (b) measured polarization distribution of deterministically fabricated devices; (c) calculated displacement for deterministically fabricated devices given the distribution from (b) and the dependence between polarization and displacement from (a). (a) Reproduced from Peniakov *et al.*, Laser Photonics Rev. **18**, 2300835 (2024). Copyright 2024 Authors licensed under a Creative Commons Attribution (CC BY) License.[116] (b) and (c) Reproduced from Buchinger *et al.*, Nano Convergence **12**, 36 (2025). Copyright 2025 Authors licensed under a Creative Commons Attribution (CC BY) License.[117]

range of the cavity resonance relaxes the wavelength matching between quantum dot and cavity so much that neither active tuning nor cherry picking needs to be used. Nevertheless, there is no free lunch. The mode volume of the CBG resonator is very small. This means that placing the resonator in arrays over randomly placed quantum dots, as it can be done with micropillars (plus some cherry picking), has an extremely low device yield and is not recommended. Furthermore, the accuracy of deterministic device placement with device placement accuracies in the hundreds of nanometer range was not accurate enough.[19,120] We learned that even small misplacements of the emitter, with respect to the cavity center creates very large polarization effects and can fully polarize the emission, see Fig. 5(a).[116] While this can also be wanted, a deterministic fully polarized device has the same demands on placement accuracy. While such an accuracy is very challenging, it can be achieved with optical imaging and e-beam lithography, when using advanced imaging correction techniques, see Figs. 5(b) and 5(c).[117,121,122]

Another advantage of the CBG resonator design is its possibility for efficient strain transfer into the emitter, which allows wavelength[19,123] and fine-structure splitting tuning,[124] which is not very effective in micropillar structures.[125] Furthermore, the CBG resonator can be tuned postprocessing to spectrally match the quantum dot emission.[126,127] These features together have enabled a series of experiments that look in detail at the properties of entangled photon pairs[128,129] and the first demonstration of teleportation of quantum information from one photon created from one quantum dot to a photon created from another quantum dot using an entangled photon pair.[130] Recently, the same device allowed for a successful entanglement swapping of photonic entanglement between photons generated from two separate devices.[131] An open challenge is the integration of CBGs with diode structures to achieve charge tunability and to suppress blinking of the emission. While there have been experimental attempts in modified structures that either sacrifice efficiency[18] or give up the low Q factor, by making very large resonators,[132] an optimized device, as suggested by Buchinger *et al.*[133] and later optimized by Prasad *et al.*[134] has not yet been demonstrated experimentally. Recently, quantum dots implemented in CBGs in the telecom C-band showed high indistinguishability of successively emitted photons.[58,135]

In addition to the above-mentioned devices, which usually create photons with emission out of the plane that can be coupled to fiber after an objective or directly,[136] for integrated devices, it is beneficial to keep the photons directly in the chip. However, on chip waveguides usually transport only one polarization, and thus encoding information in polarization, which is rather straightforward in out-of-plane cavity structures, is extremely challenging in integrated devices. Usually, a different encoding, like time-bin or path, has to be chosen in those cases. Integrating quantum dots into a DBR ridge waveguide can be used to achieve single-photon emission with near unity indistinguishability.[137] Other approaches for integrated photonics involve photonic crystal waveguides[102] that can also be used for in-plane cavities[138] and for chiral coupling of quantum dots,[139] and slab waveguides, which can be suspended,[140] on dielectric[141] or heterogeneously coupled to other waveguiding materials.[91] Under vertical excitation, the optical modes of the excitation laser and the waveguide mode are perpendicular. This allows for resonant-frequency pumping without the need for any additional cross-polarization filtering. This approach is compatible with current active and passive integrated components, such as quantum dot integration into on-chip resonators for a further Purcell-reduction of the excitonic lifetime.[142]

Photonic wire-bonding of a quantum dot distributed Bragg grating waveguide enabled a true plug-and-play fiber-coupled single-photon source, allowing resonant-frequency pumping without additional cross-polarization filtering[143] as also demonstrated in the opposite direction without wire-bonds.[144]

Outlook: Co-design, integration, and scaling of telecom-band quantum dot photonics

Telecom-band quantum dot photonics is transitioning from isolated, high-performance laboratory demonstrations to an integrated platform capable of supporting long-distance quantum networks and photonic quantum computing architectures. The defining shift that needs to happen in the near future is from optimizing individual devices to engineering reproducible, wafer-scale systems whose properties are aligned with architectural requirements. Future progress will be determined not by incremental improvements in isolated metrics, but by coordinated advances in materials growth, deterministic nanofabrication, photonic circuit integration, hybrid control techniques, and network-level functionality. In this context, five directions stand out as particularly decisive: site-controlled growth, large-scale photonic circuit integration, interfaces to quantum memories, deployment in long-distance networks, and deterministic generation of entangled

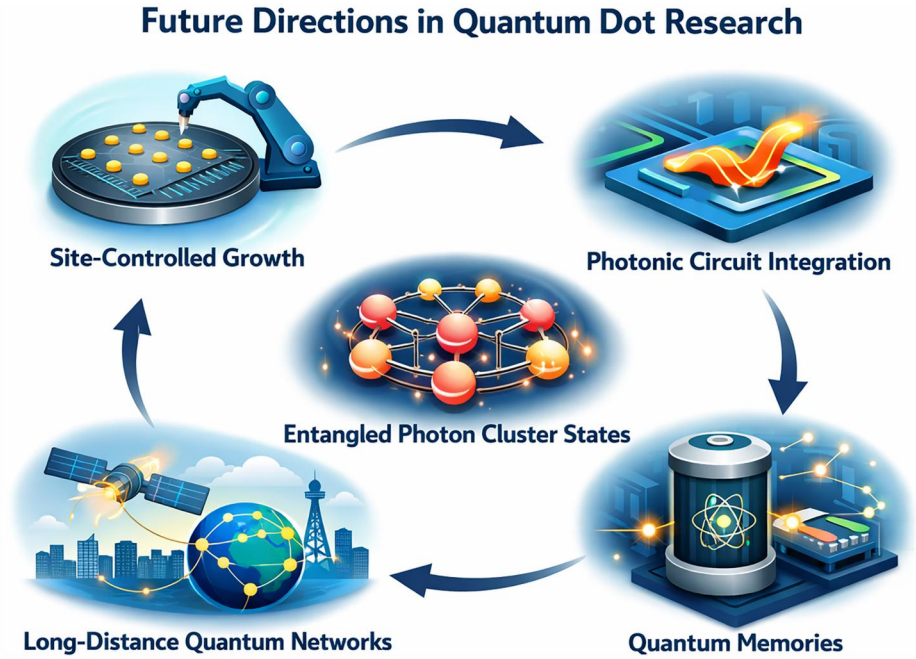

FIG. 6. Graphical representation of the future directions in quantum dot research from our personal perspective. Figure created with the help of AI. Used model: ChatGPT 5.2 (2025). Prompt to create the figure: Create a high-resolution scientific infographic titled "Future Directions in Quantum Dot Research." Layout: Landscape orientation, 16:9 ratio. Light gray background. Place five illustrated modules arranged in a circular flow, connected by large curved arrows forming a clockwise loop. Top left: A robotic arm placing yellow quantum dots on a circular semiconductor wafer. Label below: "Site-Controlled Growth" Top right: A blue photonic chip with a glowing orange wave propagating through a waveguide structure. Label: "Photonic Circuit Integration" Center: A cluster of red and orange glowing spheres connected by lines in a circular lattice pattern. Label: "Entangled Photon Cluster States" Bottom right: A cylindrical quantum memory device with an atomic symbol glowing inside, next to a small electronic chip connected by light lines. Label: "Quantum Memories" Bottom left: A globe with network nodes connected by glowing lines, a satellite in orbit, and a city skyline in the background. Label: "Long-Distance Quantum Networks" Style requirements: Semi-3D glossy vector illustration—Soft glow effects around elements—Blue dominant color scheme with orange highlights—Clean sans-serif typography—Professional journal infographic quality—Smooth shading and subtle depth use bold dark blue arrows connecting the modules in a circular progression.

photonic graph states like cluster states, 4-photon star states, 6-ring states, quantum repeater graph states or maybe other graph states that turn out to be interesting, for a graphical representation of these five directions, see Fig. 6.

Among these five directions, site-controlled quantum dot growth represents perhaps the most fundamental enabler of scalable device integration because it allows for precise placement and uniformity. Telecom-band quantum dots based on InAs/InP and related heterostructures have demonstrated near-transform-limited emission under resonant excitation and two-photon interference visibilities approaching those of shorter-wavelength GaAs systems.[135,145,146] However, present performance remains largely device-specific. Deterministic positioning with sub-10 nm spatial accuracy, narrow spectral spreads across centimeter-scale wafers, and near-unity site yield (all while preserving linewidths and indistinguishability comparable to the best self-assembled dots) would fundamentally change the fabrication paradigm. Buried stressor[147] and nanohole or pyramidal platforms[148,149] have made steady progress in spatial ordering and optical quality, but uniformity and yield must reach production-grade standards before site-controlled quantum dots can underpin large-scale circuits. At the materials level, suppressing alloy disorder, improving interface abruptness, and electrostatically quieting the heterostructure remain central to minimize spectral diffusion and charge noise. Because hyperfine interactions cannot be eliminated in III–V hosts via isotopic purification, practical strategies will continue to emphasize hole-spin approaches, nuclear feedback, operation at bias "sweet spots," and epitaxial design that stabilizes the charge environment.

Deterministic growth alone is insufficient without equally deterministic nanophotonic integration. The field is increasingly defined by fabricating the optimal nanophotonic environment (for example, a cavity or waveguide) around a pre-characterized emitter rather than searching for rare occasions of incidentally well-positioned quantum dots. Hyperspectral imaging and related wafer-scale localization techniques now allow simultaneous mapping of emitter position and spectrum with ∼15 nm total spatial uncertainty, enabling automated mask generation and device pre-selection.[117] In symmetry-sensitive structures such as circular Bragg gratings, nanometer-scale misalignment directly degrades coupling efficiency and induces polarization asymmetries,[116] turning polarization mapping into a sensitive diagnostic of placement fidelity. Similar alignment constraints apply to photonic crystal and nanobeam cavities operating at moderate quality factors,[150] where nanometer-scale precision is required to preserve Purcell enhancement and extraction efficiency. As a result, metrology, lithography, and optical design must be co-optimized as a single process chain.

Beyond single cavities, the next frontier is full photonic circuit integration. No single material platform simultaneously offers deterministic emission, low-loss routing, high-speed reconfigurability, nonlinear frequency conversion, and memory compatibility. Heterogeneous integration, therefore, becomes central. Silicon and silicon nitride photonics provide dense, programmable interferometric meshes that can transform quantum dot sources into software-defined photonic processors.[151] Thin-film lithium niobate adds low-loss electro-optic modulation[152] and χ^2 nonlinear conversion,[153] enabling high-speed feedforward and frequency translation. Hybrid demonstrations integrating multiple strain-tunable quantum dots on lithium niobate chips[154] and coupling site-controlled emitters into SiN waveguide arrays illustrate a credible path toward multi-emitter circuits with deterministic interfaces. At the packaging level, photonic wire bonding[155] and fiber-integrated modules offer alignment-tolerant, low-loss interconnects compatible with heterogeneous chip assemblies. The long-term objective is not merely on-chip extraction efficiency, but fully programmable photonic circuits in which routing, fusion operations, and feedback control are embedded within the hardware layer.

These integrated circuits must ultimately interface with quantum memories to support scalable architectures,[156,157] unless the quantum memory can be absorbed into the source of entanglement.[31] Long-distance quantum communication and distributed quantum computing require storage, synchronization, and time multiplexing of photonic qubits. Telecom-band emission is inherently compatible with fiber transmission, but memory systems (for example, atomic ensembles or rare earth elements-doped crystals) often operate at different wavelengths and bandwidths. Strain and Stark tuning of quantum dots, combined with cavity-engineered bandwidth control and on-chip nonlinear conversion, provide mechanisms for spectral matching. The integration of deterministic emitters with quantum memories would enable repeater nodes capable of entanglement swapping, buffering, and multiplexed graph-state growth. In this sense, telecom quantum dots must evolve from isolated photon sources into fully networked quantum transducers.

Long-distance quantum networks impose additional constraints beyond local device metrics. Indistinguishability must be maintained not only within a single emitter over time, but across multiple, spatially separated sources. Recent demonstrations of $\geq$90% raw two-photon interference visibility in the telecom C band confirm that high intrinsic coherence is achievable under resonant excitation and moderate Purcell enhancement, with lifetimes reduced to the sub-hundred-picosecond regime. The next step is extending this performance to multi-source interference across chips and, eventually,

Box 1. Near-future action plan for telecom band quantum dot photonics.
This roadmap organizes near-future tasks into three priority tiers that reflect dependencies, not dates. Progress at each tier unlocks subsequent tiers and should be reported using standardized device- and system-level metrics.

Priority I, foundational enablers

- **Materials and site-controlled growth:** Improve wafer-level uniformity and reduce charge-noise/spectral-diffusion baselines; advance side controlled quantum dot platforms toward sub-10 nm spatial accuracy, near-unity site-occupancy, and a few-nm spectral spreads.
- **Deterministic nanofabrication and placement:** Achieve $\leq$15–20 nm end-to-end placement into small-mode cavities; integrate hyperspectral imaging-based selection and mask autogeneration; adopt polarization-resolved cavity metrology (e.g., in CBGs) as a placement acceptance test.
- **Symmetry-preserving tuning:** Co-design electrical, strain, and post-fabrication cavity tuning so both quantum dot and cavity remain stable and polarization-balanced; validate low-loss contacts for CBGs; standardize post-fabrication trimming of photonic components for deterministic resonance alignment/correction.

Priority II, device-level robustness and multi-photon capability

- **Reproducible coherence and indistinguishability:** Produce device batches with $\geq$90 % two-photon indistinguishability (raw, resonant); report wafer-level resonant linewidth histograms, charge-noise spectra, and time-resolved spectral-diffusion statistics.
- **Deterministic multi-photon readiness:** Demonstrate telecom spin–photon and spin–photon–photon entanglement with FSS $< 1\ \mu$eV under hybrid strain+electrical tuning; use moderate-Q Purcell to reach $<$100 ps lifetimes without spectral-filtering penalties.
- **Hybrid stabilization:** Implement closed-loop feedback (strain for slow drifts, electrical for fast fluctuations); introduce automated device-qualification metrics (polarization symmetry, indistinguishability, Δ-detuning stability).

Priority III—Scaling, integration and photonic architectures

- **Multi-source operation:** Realize reliable two-source C-band interference on-chip via per-device tuning and synchronized excitation; engineer array-level lifetime uniformity and matched temporal envelopes.
- **Heterogeneous integration:** Combine deterministic quantum dots with LN/Si photonic processors for routing/modulation; evaluate photonic-wire-bonding (or equivalent) for low-loss chip-to-chip links; enable software-based emitter selection from large arrays.
- **Toward fault-tolerant systems:** Incorporate programmable interferometric meshes, fusion-gate primitives, and active stabilization; define and report system-level KPIs (inter-source matching bandwidth, cross-device coherence stability, drift tolerance, array uniformity, and packaging-loss budgets).

across nodes. Achieving this requires wafer-level reproducibility of linewidths under resonant drive, quantitative characterization of spectral diffusion and charge noise spectra, and closed-loop stabilization combining electrical bias, strain tuning, and post-fabrication cavity trimming. Electrical control stabilizes charge states and enables Stark alignment over several nanometers, while strain tuning suppresses fine-structure splitting and preserves polarization symmetry, which is an essential condition for entanglement distribution over fiber. When combined with low-loss interconnects and programmable photonic routing, these capabilities lay the groundwork for repeater-grade quantum links operating directly in the telecom band.

Perhaps the most transformative application of telecom band quantum dots lies in deterministic generation of entangled photon cluster states. Unlike probabilistic downconversion sources, quantum dot spins enable sequential emission of entangled photons at hundreds of MHz repetition rates, forming one-dimensional cluster states suitable for measurement-based quantum computing and fusion-based architectures. Near-infrared systems have already demonstrated strings of approximately ten indistinguishable photons, validating the protocol. Initial spin coherence measurements and spin–photon entanglement demonstrations at 1550 nm establish the essential ingredients in the telecom band.[158,159] Extending cluster length and fidelity requires long spin coherence across repeated emission cycles, stable suppression of fine-structure splitting, and high photon indistinguishability without flux-reducing spectral filtering.[24,30] Here, materials improvements, hybrid electrical–mechanical control, and moderate-Q Purcell enhancement converge directly on architectural requirements. In a network context, cluster states distributed over long fiber links could enable measurement-based repeater schemes and distributed photonic computing.

Taken together, these directions signal a transition to a systems-level era of telecom quantum dot photonics. Site-controlled growth must deliver spatial and spectral determinism at the wafer scale. Photonic circuit integration must embed emitters into programmable, low-loss architectures. Quantum memory interfaces must provide storage and synchronization for multiplexed operations. Long-distance networks demand reproducible indistinguishability and polarization-stable entanglement distribution. Deterministic cluster-state generation must translate single-spin coherence into scalable graph states. The central challenge is no longer whether individual components can achieve state-of-the-art performance, but how rapidly these components can be merged into a reproducible, protocol-aware quantum photonic platform. As this convergence accelerates, telecom quantum dots will evolve from high-quality single-photon sources into network-ready quantum state generators capable of supporting entanglement distribution over metropolitan and intercity scales, as well as scalable photonic quantum computing architectures. In Box 1, we summarize possible future directions of Telecom Band quantum dot photonics.

CONCLUSION

Semiconductor quantum dots are promising sources of single and entangled photons for quantum technologies due to their low multi-photon contribution, usually in the 1% range, high photon flux, and scalability. Yet, this technology also faces some issues in the form of a relatively low binding energy and high optical refractive indices, which necessitate cooling to cryogenic temperatures and engineering the nanophotonic environment.

This review examines device-level strategies to optimize quantum dot emission performance, with a focus on the recent contributions from the University of Würzburg. Key developments include epitaxial growth, charge control, piezo-tuning, and photonic integration using micropillars and circular Bragg gratings. These developments are facilitated by advances in hyperspectral imaging, which allows for deterministic device integration of individual dots into tailor-fit nanophotonic components. Advances in near-infrared quantum dot single-photon sources and in the photon indistinguishability in the telecom C-band, where techniques like cavity-enhanced emission and resonant excitation have improved the performance of quantum dot single-photon sources, are discussed. These efforts highlight the potential of quantum dots in enabling secure communication, quantum networks, and quantum computing.

ACKNOWLEDGMENTS

The authors acknowledge the support of the state of Bavaria and the Federal Ministry of Research, Technology, and Space (BMFTR) within Projects PhotonQ (Grant No. FKZ: 13N15759), QuNET+ICLink (Grant No. FKZ: 16KIS1975), PoQuaHonta (Grant No. FKZ: 13N16982), QR.X (Grant No. FKZ: 16KISQ010), and QR.N (Grant No. FKZ: 16KIS2209).

Tobias Huber-Loyola acknowledges financial support from the BMFTR within the Project Qecs (Grant No. FKZ: 13N16272).

The authors thank Reza Hekmati for proofreading the final manuscript.

AUTHOR DECLARATIONS

Conflict of Interest

The authors have no conflicts to disclose.

Author Contributions

Tobias Huber-Loyola: Conceptualization (equal); Visualization (equal); Writing – original draft (equal); Writing – review & editing (equal). **Andreas Pfenning:** Conceptualization (supporting); Writing – original draft (supporting); Writing – review & editing (supporting). **Johannes Michl:** Visualization (equal); Writing – original draft (equal). **Sven Höfling:** Writing – original draft (supporting); Writing – review & editing (lead).

DATA AVAILABILITY

Data sharing is not applicable to this article as no new data were created or analyzed in this study.

REFERENCES

[1]P. Senellart, G. Solomon, and A. White, "High-performance semiconductor quantum-dot single-photon sources," Nat. Nanotechnol. **12**, 1026–1039 (2017).
[2]X. Zhou, L. Zhai, and J. Liu, "Epitaxial quantum dots: A semiconductor launchpad for photonic quantum technologies," Photonics Insights **1**, R07 (2022).
[3]C. Schimpf *et al.*, "Quantum dots as potential sources of strongly entangled photons: Perspectives and challenges for applications in quantum networks," Appl. Phys. Lett. **118**, 100502 (2021).
[4]C. P. Dietrich, A. Fiore, M. G. Thompson, M. Kamp, and S. Höfling, "GaAs integrated quantum photonics: Towards compact and multi-functional

quantum photonic integrated circuits," Laser Photonics Rev. **10**, 870–894 (2016).
[5]X. Ding *et al.*, "On-demand single photons with high extraction efficiency and near-unity indistinguishability from a resonantly driven quantum dot in a micropillar," Phys. Rev. Lett. **116**, 020401 (2016).
[6]H. Wang *et al.*, "On-demand semiconductor source of entangled photons which simultaneously has high fidelity, efficiency, and indistinguishability," Phys. Rev. Lett. **122**, 113602 (2019).
[7]M. Müller, S. Bounouar, K. D. Jöns, M. Glässl, and P. Michler, "On-demand generation of indistinguishable polarization-entangled photon pairs," Nat. Photonics **8**, 224–228 (2014).
[8]N. Akopian *et al.*, "Entangled photon pairs from semiconductor quantum dots," Phys. Rev. Lett. **96**, 130501 (2006).
[9]M. Gurioli, Z. Wang, A. Rastelli, T. Kuroda, and S. Sanguinetti, "Droplet epitaxy of semiconductor nanostructures for quantum photonic devices," Nat. Mater. **18**, 799–810 (2019).
[10]Y. Yu *et al.*, "Telecom-band quantum dot technologies for long-distance quantum networks," Nat. Nanotechnol. **18**, 1389–1400 (2023).
[11]F. Olbrich *et al.*, "Polarization-entangled photons from an InGaAs-based quantum dot emitting in the telecom C-band," Appl. Phys. Lett. **111**, 133106 (2017).
[12]G. Juska, V. Dimastrodonato, L. O. Mereni, A. Gocalinska, and E. Pelucchi, "Towards quantum-dot arrays of entangled photon emitters," Nat. Photonics **7**, 527–531 (2013).
[13]S. Maier *et al.*, "Site-controlled InAs/GaAs quantum dots emitting at telecommunication wavelength," Semicond. Sci. Technol. **29**, 052001 (2014).
[14]H. Z. Song *et al.*, "Site-controlled photoluminescence at telecommunication wavelength from InAs/InP quantum dots," Appl. Phys. Lett. **86**, 113118 (2005).
[15]C. Schneider *et al.*, "Single site-controlled In(Ga)As/GaAs quantum dots: Growth, properties and device integration," Nanotechnology **20**, 434012 (2009).
[16]C. Kistner *et al.*, "Demonstration of strong coupling via electro-optical tuning in high-quality QD-micropillar systems," Opt. Express **16**, 15006–15012 (2008).
[17]M. Moczała-Dusanowska *et al.*, "Strain-tunable single-photon source based on a quantum dot–micropillar system," ACS Photonics **6**, 2025–2031 (2019).
[18]S. Wijitpatima *et al.*, "Bright electrically contacted circular Bragg grating resonators with deterministically integrated quantum dots," ACS Nano **18**, 31834–31845 (2024).
[19]M. Moczała-Dusanowska *et al.*, "Strain-tunable single-photon source based on a circular Bragg grating cavity with embedded quantum dots," ACS Photonics **7**, 3474–3480 (2020).
[20]C. Couteau *et al.*, "Applications of single photons in quantum metrology, biology and the foundations of quantum physics," Nat. Rev. Phys. **5**, 354–363 (2023).
[21]C. Couteau *et al.*, "Applications of single photons to quantum communication and computing," Nat. Rev. Phys. **5**, 326–338 (2023).
[22]P. Holewa *et al.*, "Solid-state single-photon sources operating in the telecom wavelength range," Nanophotonics **14**, 1729 (2025).
[23]J. M. Zajac, R. Hekmati, T. Huber-Loyola, and S. Hofling, "Quantum dots for quantum repeaters," arXiv:2503.13775v2 [quant-ph] (2025). http://arxiv.org/pdf/2503.13775.
[24]D. Cogan, Z.-E. Su, O. Kenneth, and D. Gershoni, "Deterministic generation of indistinguishable photons in a cluster state," Nat. Photonics **17**, 324–329 (2023).
[25]N. H. Lindner and T. Rudolph, "Proposal for pulsed on-demand sources of photonic cluster state strings," Phys. Rev. Lett. **103**, 113602 (2009).
[26]I. Schwartz *et al.*, "Deterministic generation of a cluster state of entangled photons," Science **354**, 434–437 (2016).
[27]N. Coste *et al.*, "High-rate entanglement between a semiconductor spin and indistinguishable photons," Nat. Photonics **17**, 582–587 (2023).
[28]S. C. Wein *et al.*, "Minimizing resource overhead in fusion-based quantum computation using hybrid spin-photon devices," PRX Quantum **6**, 040362 (2025).
[29]Y. Reum *et al.*, "Deterministic entanglement as a prerequisite for scalable quantum photonic resource state generation," Adv. Quantum Technol. (in press).
[30]R. Prasad *et al.*, "Analytical fidelity calculations for photonic linear cluster state generation," Nano Convergence **12**, 44 (2025).
[31]K. Azuma, K. Tamaki, and H.-K. Lo, "All-photonic quantum repeaters," Nat. Commun. **6**, 6787 (2015).
[32]S. Bartolucci *et al.*, "Fusion-based quantum computation," Nat. Commun. **14**, 912 (2023).
[33]P. Loock *et al.*, "Extending quantum links: Modules for fiber- and memory-based quantum repeaters," Adv. Quantum Technol. **3**, 1900141 (2020).
[34]P. Thomas, L. Ruscio, O. Morin, and G. Rempe, "Efficient generation of entangled multiphoton graph states from a single atom," Nature **608**, 677–681 (2022).
[35]P. Thomas, L. Ruscio, O. Morin, and G. Rempe, "Fusion of deterministically generated photonic graph states," Nature **629**, 567–572 (2024).
[36]K. Tiurev *et al.*, "High-fidelity multiphoton-entangled cluster state with solid-state quantum emitters in photonic nanostructures," Phys. Rev. A **105**, 030601 (2022).
[37]D. Bauch, N. Köcher, N. Heinisch, and S. Schumacher, "Time-bin entanglement in the deterministic generation of linear photonic cluster states," APL Quantum **1**, 036110 (2024).
[38]N. Tomm *et al.*, "A bright and fast source of coherent single photons," Nat. Nanotechnol. **16**, 399–403 (2021).
[39]X. Ding *et al.*, "High-efficiency single-photon source above the loss-tolerant threshold for efficient linear optical quantum computing," Nat. Photonics **19**, 387–391 (2025).
[40]J. Neuwirth *et al.*, "Multipair-free source of entangled photons in the solid state," Phys. Rev. B **106**, 241402 (2022).
[41]A. Y. Cho and H. C. Casey, Jr., "GaAs–Al_x Ga_{1-x} As double-heterostructure lasers prepared by molecular-beam epitaxy," Appl. Phys Lett **25**, 288–290 (1974).
[42]A. I. Ekimov and A. A. Onushchenko, "Quantum size effect in three-dimensional microscopic semiconductor crystals," JETP **34**, 363 (1981).
[43]Y. Arakawa and H. Sakaki, "Multidimensional quantum well laser and temperature dependence of its threshold current," Appl. Phys. Lett. **40**(11), 939–941 (1982).
[44]L. Goldstein, F. Glas, J. Y. Marzin, M. N. Charasse, and G. Le Roux, "Growth by molecular beam epitaxy and characterization of InAs/GaAs strained-layer superlattices," Appl. Phys. Lett. **47**(10), 1099–1101 (1985).
[45]D. Leonard, M. Krishnamurthy, C. M. Reaves, S. P. Denbaars, and P. M. Petroff, "Direct formation of quantum-sized dots from uniform coherent islands of InGaAs on GaAs surfaces," Appl. Phys. Lett. **63**, 3203–3205 (1993).
[46]C. Becher *et al.*, "Nonclassical radiation from a single self-assembled InAs quantum dot," Phys. Rev. B **63**, 121312 (2001).
[47]P. Michler, A. Kiraz, C. Becher, W. V. Schoenfeld, P. M. Petroff, L. Zhang, E. Hu, and A. Imamoglu, "A quantum dot single-photon turnstile device," Science **290**(5500), 2282–2285 (2000).
[48]P. Michler, A. Imamoğlu, M. D. Mason, P. J. Carson, G. F. Strouse, and S. K. Buratto, "Quantum correlation among photons from a single quantum dot at room temperature," Nature **406**(6799), 968–970 (2000).
[49]T. Yoshie *et al.*, "Vacuum Rabi splitting with a single quantum dot in a photonic crystal nanocavity," Nature **432**, 200–203 (2004).
[50]K. Hennessy *et al.*, "Quantum nature of a strongly coupled single quantum dot–cavity system," Nature **445**, 896–899 (2007).
[51]D. Englund *et al.*, "Controlling the spontaneous emission rate of single quantum dots in a two-dimensional photonic crystal," Phys. Rev. Lett. **95**, 013904 (2005).
[52]N. Somaschi *et al.*, "Near-optimal single-photon sources in the solid state," Nat. Photonics **10**, 340–345 (2016).
[53]S. Unsleber *et al.*, "Highly indistinguishable on-demand resonance fluorescence photons from a deterministic quantum dot micropillar device with 74% extraction efficiency," Opt. Express **24**, 8539–8546 (2016).
[54]C. Böckler *et al.*, "Electrically driven high-Q quantum dot-micropillar cavities," Appl. Phys. Lett. **92**, 091107 (2008).
[55]C. Nawrath *et al.*, "Bright Source of Purcell-Enhanced, Triggered, Single Photons in the Telecom C-Band," Adv. Quantum Tech. **6**, 2300111 (2023).
[56]P. Holewa *et al.*, "High-throughput quantum photonic devices emitting indistinguishable photons in the telecom C-band," Nat. Commun. **15**, 3358 (2024).
[57]J. Kaupp *et al.*, "Purcell-enhanced single-photon emission in the telecom C-band," Adv. Quantum Technol. **6**, 2300242 (2023).

[58]J. Kim *et al.*, "Two-photon interference from an InAs quantum dot emitting in the telecom C-band," Adv. Quantum Technol. **8**, 2500069 (2025).
[59]M. Fatemeh and J. Stride, "A brief review on core/shell quantum dots," SDRP J. Nanotechnol. Mater. Sci. **3**, 121–126 (2020).
[60]J. M. García, T. Mankad, P. O. Holtz, P. J. Wellman, and P. M. Petroff, "Electronic states tuning of InAs self-assembled quantum dots," Appl. Phys. Lett. **72**, 3172–3174 (1998).
[61]L. Wang, A. Rastelli, and O. G. Schmidt, "Structural and optical properties of In(Ga)As/GaAs quantum dots treated by partial capping and annealing," J. Appl. Phys. **100**, 064313 (2006).
[62]D. Fuster *et al.*, "Direct formation of InAs quantum dots grown on InP (001) by solid-source molecular beam epitaxy," Appl. Phys. Lett. **94**, 133106 (2009).
[63]M. Benyoucef, M. Yacob, J. P. Reithmaier, J. Kettler, and P. Michler, "Telecom-wavelength (1.5 μm) single-photon emission from InP-based quantum dots," Appl. Phys. Lett. **103**, 162101 (2013).
[64]D. Cooper *et al.*, "Quantitative strain mapping of InAs/InP quantum dots with 1 nm spatial resolution using dark field electron holography," Appl. Phys. Lett. **99**, 261911 (2011).
[65]S. Fafard, Z. Wasilewski, J. McCaffrey, S. Raymond, and S. Charbonneau, "InAs self-assembled quantum dots on InP by molecular beam epitaxy," Appl. Phys. Lett. **68**, 991–993 (1996).
[66]S. Fréchengues *et al.*, "Wavelength tuning of InAs quantum dots grown on (311)B InP," Appl. Phys. Lett. **74**, 3356–3358 (1999).
[67]B. Salem *et al.*, "Optical properties of self-assembled InAs quantum islands grown on InP(001) vicinal substrates," Appl. Phys. Lett. **79**, 4435–4437 (2001).
[68]O. Bierwagen and W. T. Masselink, "Self-organized growth of InAs quantum wires and dots on InP(001): The role of vicinal substrates," Appl. Phys. Lett. **86**, 113110 (2005).
[69]E. S. Semenova *et al.*, "Metamorphic approach to single quantum dot emission at 1.55 μm on GaAs substrate," J. Appl. Phys. **103**, 103533 (2008).
[70]S. L. Portalupi, M. Jetter, and P. Michler, "InAs quantum dots grown on metamorphic buffers as non-classical light sources at telecom C-band: A review," Semicond. Sci. Technol. **34**, 053001 (2019).
[71]M. Sundaram, A. Wixforth, R. S. Geels, A. C. Gossard, and J. H. English, "A direct method to produce and measure compositional grading in $Al_xGa_{1-x}As$ alloys," J. Vac. Sci. Technol. B **9**, 1524–1529 (1991).
[72]L. G. Vaughn, L. Ralph, H. Xu, Y. Jiang, and L. F. Lester, "Characterization of AlInAsSb and AlGaInAsSb MBE-grown digital alloys," MRS Online Proc. Libr. **744**, 72 (2003).
[73]A. C. Gossard, P. M. Petroff, W. Weigmann, R. Dingle, and A. Savage, "Epitaxial structures with alternate-atomic-layer composition modulation," Appl. Phys. Lett. **29**, 323–325 (1976).
[74]N. Bart *et al.*, "Wafer-scale epitaxial modulation of quantum dot density," Nat. Commun. **13**, 1633 (2022).
[75]P. M. Petroff, "Epitaxial growth and electronic structure of self-assembled quantum dots," in *Single Quantum Dots* (Springer, 2003), Vol. **90**, pp. 1–24.
[76]J. C. Loredo *et al.*, "Scalable performance in solid-state single-photon sources," Optica **3**, 433 (2016).
[77]G. Bucci *et al.*, "Zincblende $InAs_xP_{1-x}$/InP quantum dot nanowires for telecom wavelength emission," ACS Appl. Mater. Interfaces **16**, 26491–26499 (2024).
[78]M. T. Borgström, V. Zwiller, E. Müller, and A. Imamoglu, "Optically bright quantum dots in single Nanowires," Nano Lett. **5**, 1439–1443 (2005).
[79]J. Heinrich *et al.*, "Single photon emission from positioned GaAs/AlGaAs photonic nanowires," Appl. Phys. Lett. **96**, 211117 (2010).
[80]L. Wells *et al.*, "Coherent light scattering from a telecom C-band quantum dot," Nat. Commun. **14**, 8371 (2023).
[81]C. Heyn *et al.*, "Single-dot spectroscopy of GaAs quantum dots fabricated by filling of self-assembled nanoholes," Nanoscale Res. Lett. **5**, 1633–1636 (2010).
[82]A. Chellu, J. Hilska, J.-P. Penttinen, and T. Hakkarainen, "Highly uniform GaSb quantum dots with indirect–direct bandgap crossover at telecom range," APL Mater. **9**, 051116 (2021).
[83]G. N. Nguyen *et al.*, "Enhanced electron-spin coherence in a GaAs quantum emitter," Phys. Rev. Lett. **131**, 210805 (2023).
[84]M. H. Appel *et al.*, "A many-body quantum register for a spin qubit," Nat. Phys. **21**, 368–373 (2025).
[85]D. M. Jackson *et al.*, "Optimal purification of a spin ensemble by quantum-algorithmic feedback," Phys. Rev. X **12**, 031014 (2022).
[86]L. Zaporski *et al.*, "Ideal refocusing of an optically active spin qubit under strong hyperfine interactions," Nat. Nanotechnol. **18**, 257–263 (2023).
[87]J. Michl *et al.*, "Strain-free GaSb quantum dots as single-photon sources in the telecom S-band," Adv. Quantum Tech. **6**, 2300180 (2023).
[88]I. M. Masson *et al.*, "Engineering nanohole-etched quantum dots for telecom-band single-photon generation," ACS Nano **20**, 2872–2880 (2026).
[89]T. Heindel *et al.*, "Electrically driven quantum dot-micropillar single photon source with 34% overall efficiency," Appl. Phys. Lett. **96**, 011107 (2010).
[90]M. Arcari *et al.*, "Near-unity coupling efficiency of a quantum emitter to a photonic crystal waveguide," Phys. Rev. Lett. **113**, 093603 (2014).
[91]M. Davanco *et al.*, "Heterogeneous integration for on-chip quantum photonic circuits with single quantum dot devices," Nat. Commun. **8**, 889 (2017).
[92]J. Gérard *et al.*, "Enhanced spontaneous emission by quantum boxes in a monolithic optical microcavity," Phys. Rev. Lett. **81**, 1110–1113 (1998).
[93]J. P. Reithmaier *et al.*, "Strong coupling in a single quantum dot-semiconductor microcavity system," Nature **432**, 197–200 (2004).
[94]E. M. Purcell, "Spontaneous emission probabilities at radio frequencies," Phys. Rev. **69**, 674 (1946).
[95]C. Weisbuch, M. Nishioka, A. Ishikawa, and Y. Arakawa, "Observation of the coupled exciton-photon mode splitting in a semiconductor quantum microcavity," Phys. Rev. Lett. **69**, 3314–3317 (1992).
[96]E. Yablonovitch, "Inhibited spontaneous emission in solid-state physics and electronics," Phys. Rev. Lett. **58**, 2059–2062 (1987).
[97]S. John, "Strong localization of photons in certain disordered dielectric superlattices," Phys. Rev. Lett. **58**, 2486–2489 (1987).
[98]Y. Akahane, T. Asano, B.-S. Song, and S. Noda, "High-Q photonic nanocavity in a two-dimensional photonic crystal," Nature **425**, 944–947 (2003).
[99]M. Nomura, Y. Ota, N. Kumagai, S. Iwamoto, and Y. Arakawa, "Large vacuum rabi splitting in single self-assembled quantum dot-nanocavity system," Appl. Phys. Express **1**, 072102 (2008).
[100]A. Reinhard *et al.*, "Strongly correlated photons on a chip," Nat. Photonics **6**, 93–96 (2012).
[101]F. Liu *et al.*, "High Purcell factor generation of indistinguishable on-chip single photons," Nat. Nanotech. **13**, 835–840 (2018).
[102]T. Lund-Hansen *et al.*, "Experimental realization of highly efficient broadband coupling of single quantum dots to a photonic crystal waveguide," Phys. Rev. Lett. **101**, 113903 (2008).
[103]T. B. Hoang *et al.*, "Widely tunable, efficient on-chip single photon sources at telecommunication wavelengths," Opt. Express **20**, 21758–21765 (2012).
[104]P. Lodahl, S. Mahmoodian, and S. Stobbe, "Interfacing single photons and single quantum dots with photonic nanostructures," Rev. Mod. Phys. **87**, 347–400 (2015).
[105]A. S. Sheremet, M. I. Petrov, I. V. Iorsh, A. V. Poshakinskiy, and A. N. Poddubny, "Waveguide quantum electrodynamics: Collective radiance and photon-photon correlations," Rev. Mod. Phys. **95**, 015002 (2023).
[106]S. Frédérick *et al.*, "InAs/InP quantum dot photonic crystal microcavities," Phys. Status Solidi (c) **3**, 3685–3688 (2006).
[107]B. Zhang *et al.*, "Fabrication of InAs quantum dots in AlAs/GaAs DBR pillar microcavities for single photon sources," J. Appl. Phys. **97**, 073507 (2005).
[108]L. Ginés *et al.*, "High extraction efficiency source of photon pairs based on a quantum dot embedded in a broadband micropillar cavity," Phys. Rev. Lett. **129**, 033601 (2022).
[109]A. D. Osterkryger, J. Claudon, J.-M. Gérard, and N. Gregersen, "Photonic "hourglass" design for efficient quantum light emission," Opt. Lett. **44**, 2617 (2019).
[110]J. Jurkat *et al.*, "Technological implementation of a photonic Bier-Glas cavity," Phys. Rev. Mater. **5**, 064603 (2021).
[111]L. Ginés *et al.*, "Time-bin entangled photon pairs from quantum dots embedded in a self-aligned cavity," Opt. Express **29**, 4174–4180 (2021).
[112]L. Engel *et al.*, "Purcell enhanced single-photon emission from a quantum dot coupled to a truncated Gaussian microcavity," Appl. Phys. Lett. **122**, 043503 (2023).
[113]S. E. Thomas *et al.*, "Deterministic storage and retrieval of telecom light from a quantum dot single-photon source interfaced with an atomic quantum memory," Sci. Adv. **10**, 211117 (2024).
[114]Ł. Dusanowski *et al.*, "Optical charge injection and coherent control of a quantum-dot spin-qubit emitting at telecom wavelengths," Nat. Commun. **13**, 748 (2022).

[115]G. Peniakov, "Initialization of neutral and charged exciton spin states in a telecom-emitting quantum dot," Phys. Rev. B **112**, 085422 (2025).
[116]G. Peniakov *et al.*, "Polarized and unpolarized emission from a single emitter in a bullseye resonator," Laser Photonics Rev. **18**, 2300835 (2024).
[117]Q. Buchinger *et al.*, "Deterministic quantum dot cavity placement using hyperspectral imaging with high spatial accuracy and precision," Nano Convergence **12**, 36 (2025).
[118]J. Scheuer and A. Yariv, "Annular Bragg defect mode resonators," J. Opt. Soc. Am. B **20**, 2285–2291 (2003).
[119]M. Davanço, M. T. Rakher, D. Schuh, A. Badolato, and K. Srinivasan, "A circular dielectric grating for vertical extraction of single quantum dot emission," Appl. Phys. Lett. **99**, 041102 (2011).
[120]Y.-M. He *et al.*, "Deterministic implementation of a bright, on-demand single photon source with near-unity indistinguishability via quantum dot imaging," Optica **4**, 802–808 (2017).
[121]C. R. Copeland *et al.*, "Traceable localization enables accurate integration of quantum emitters and photonic structures with high yield," Opt. Quantum **2**, 72 (2024).
[122]S. Liu, K. Srinivasan, and J. Liu, "Nanoscale positioning approaches for integrating single solid-state quantum emitters with photonic nanostructures," Laser Photonics Rev. **15**, 2100223 (2021).
[123]I. Gamov *et al.*, "Enhanced spectral range of strain-induced tuning of quantum dots in circular Bragg grating cavities," Advanced Quantum Technologies **9**(3), Art.-Nr.: e00954 (2026).
[124]M. B. Rota *et al.*, "A source of entangled photons based on a cavity-enhanced and strain-tuned GaAs quantum dot," eLight **4**, 13 (2024).
[125]S. Gerhardt *et al.*, "Optomechanical tuning of the polarization properties of micropillar cavity systems with embedded quantum dots," Phys. Rev. B **101**, 245308 (2020).
[126]T. M. Krieger *et al.*, "Post-fabrication tuning of circular Bragg resonators for enhanced emitter-cavity coupling," ACS Photonics **11**, 596 (2024).
[127]J. Kaupp *et al.*, "Post-fabrication tuning of circular Bragg grating resonators via atomic layer deposition," Appl. Phys. Lett. **127**, 133501 (2025).
[128]F. Basso Basset *et al.*, "Signatures of the optical stark effect on entangled photon pairs from resonantly pumped quantum dots," Phys. Rev. Lett. **131**, 166901 (2023).
[129]A. Laneve *et al.*, "Wavevector-resolved polarization entanglement from radiative cascades," Nat. Commun. **16**, 6209 (2025).
[130]A. Laneve *et al.*, "Quantum teleportation with dissimilar quantum dots over a hybrid quantum network," Nat. Commun. **16**, 10028 (2025).
[131]M. Beccaceci *et al.*, "All-photonic entanglement swapping with remote quantum dots," arXiv:2512.10651 (2025).
[132]H. Singh *et al.*, "Optical transparency induced by a largely purcell enhanced quantum dot in a polarization-degenerate cavity," Nano Lett. **22**, 7959–7964 (2022).
[133]Q. Buchinger, S. Betzold, S. Höfling, and T. Huber-Loyola, "Optical properties of circular Bragg gratings with labyrinth geometry to enable electrical contacts," Appl. Phys. Lett. **122**, 111110 (2023).
[134]R. Prasad *et al.*, "High-performance labyrinth circular Bragg grating design for charge and stark-tunable quantum light sources spanning visible to telecom wavelengths," Opt. Express **34**(8), 15100–15109 (2026).
[135]N. Hauser *et al.*, "Deterministic and highly indistinguishable single photons in the telecom C-band," Nat. Commun. **17**, 537 (2026).
[136]L. Bremer *et al.*, "Numerical optimization of single-mode fiber-coupled single-photon sources based on semiconductor quantum dots," Opt. Express **30**, 15913 (2022).
[137]Ł. Dusanowski, D. Köck, C. Schneider, and S. Höfling, "On-chip Hong–Ou–Mandel interference from separate quantum dot emitters in an integrated circuit," ACS Photonics **10**, 2941–2947 (2023).
[138]F. S. F. Brossard *et al.*, "Strongly coupled single quantum dot in a photonic crystal waveguide cavity," Appl. Phys. Lett. **97**, 111101 (2010).
[139]M. J. Mehrabad *et al.*, "Chiral topological photonics with an embedded quantum emitter," Optica **7**, 1690–1696 (2020).
[140]S. Koseki, B. Zhang, K. De Greve, and Y. Yamamoto, "Monolithic integration of quantum dot containing microdisk microcavities coupled to air-suspended waveguides," Appl. Phys. Lett. **94**, 051110 (2009).
[141]A. Shadmani *et al.*, "Integration of GaAs waveguides on a silicon substrate for quantum photonic circuits," Opt. Express **30**, 37595–37602 (2022).
[142]Ł. Dusanowski *et al.*, "Purcell-enhanced and indistinguishable single-photon generation from quantum dots coupled to on-chip integrated ring resonators," Nano Lett. **20**, 6357–6363 (2020).
[143]M. Gregorio *et al.*, "Plug-and-play fiber-coupled quantum dot single-photon source via photonic wire bonding," Adv. Quantum Technol. **7**, 2300227 (2023).
[144]T. Huber *et al.*, "Filter-free single-photon quantum dot resonance fluorescence in an integrated cavity-waveguide device," Optica **7**, 380 (2020).
[145]A. N. Wakileh *et al.*, "Approaching transform-limited linewidths in telecom-wavelength transitions of ungated quantum dots," arXiv:2509.02320 (2025).
[146]R. Behrends *et al,*" Highly-indistinguishable single-photons at 1550 nm from a two-photon resonantly excited purcell-enhanced quantum dot," arXiv:2602.06140 (2026).
[147]M. Podhorský *et al.*, "Buried stressor engineering for position-controlled InGaAs quantum dots with local density variation for integrated quantum photonics," ACS Photonics **13**, 471–481 (2026).
[148]E. Pelucchi, S. Watanabe, K. Leifer, B. Dwir, and E. Kapon, "Site-controlled quantum dots grown in inverted pyramids for photonic crystal applications," Phys. E **23**, 476–481 (2004).
[149]R. A. Barcan *et al.*, "Trion quantum coherence in site-controlled pyramidal InGaAs quantum dots," Sci. Rep. **16**, 4114 (2026).
[150]P. Lodahl *et al.*, "Chiral quantum optics," Nature **541**, 473–480 (2017).
[151]L. S. Madsen *et al.*, "Quantum computational advantage with a programmable photonic processor," Nature **606**, 75–81 (2022).
[152]A. J. Mercante *et al.*, "Thin film lithium niobate electro-optic modulator with terahertz operating bandwidth," Opt. Express **26**, 14810–14816 (2018).
[153]J. Zhao, C. Ma, M. Rüsing, and S. Mookherjea, "High quality entangled photon pair generation in periodically poled thin-film lithium niobate waveguides," Phys. Rev. Lett. **124**, 163603 (2020).
[154]X. Wang *et al.,* "Large-scale quantum-dot-lithium-niobate hybrid integrated photonic circuits enabling on-chip quantum networking," arXiv:2503.23755 (2025).
[155]N. Lindenmann *et al.*, "Photonic wire bonding: A novel concept for chip-scale interconnects," Opt. Express **20**, 17667–17677 (2012).
[156]H.-J. Briegel, W. Dür, J. I. Cirac, and P. Zoller, "Quantum repeaters: The role of imperfect local operations in quantum communication," Phys. Rev. Lett. **81**, 5932–5935 (1998).
[157]H. J. Kimble, "The quantum internet," Nature **453**, 1023–1030 (2008).
[158]J. M. Michl *et al.*, "A spin-photon interface in the telecom C-band with long hole spin dephasing time," arXiv:2512.19561v1 (2025).
[159]P. Laccotripes *et al.*, "Spin-photon entanglement with direct photon emission in the telecom C-band," Nat. Commun. **15**, 9740 (2024).